Journal of the European Ceramic Society **18** (1997) 1053–1057

PII: S0955-2219(97)00135-0
0955-2219/98/$19.00 + 0.00

Elongated α-Sialon Grains in Pressureless Sintered Sialon Ceramics

H. Zhao, S. P. Swenser and Y.-B. Cheng*

Department of Materials Engineering, Monash University, Melbourne, Victoria, 3168, Australia

(Received 18 April 1997; accepted 3 July 1997)

Abstract

Calcium α-sialons, containing elongated grains, were developed by pressureless sintering. Preliminary electron microscopy analyses revealed the high aspect ratio of the α′ grains resulted from preferred crystal growth in the [0 0 1] direction. Such grain morphologies offer hope for in-situ toughening of α-sialon materials via the promotion of crack deflection and bridging during failure. © *1998 Published by Elsevier Science Limited. All rights reserved*

Introduction

The Ca α-sialon (α′) phase is a solid solution based upon the α-Si_3N_4 crystal structure. The formula for this phase is $Ca_{m/2}Si_{12-(m+n)}Al_{(m+n)}O_nN_{16-n}$. It indicates that m (Al–N) and n (Al–O) bonds replace $(m+n)$ (Si–N) bonds. The added substitution of $(m/2)$ Ca^{2+} cations into lattice interstices compensates for the charge imbalance created by the replacement of m (Si–N) by m (Al–N) bonds. Calcium α-sialon ceramics offer several benefits over their rare-earth counterparts.

Calcium carbonate is a significantly cheaper and more abundant resource than the rare-earth oxides. The lower melting points of the Ca-containing systems facilitate densification at reduced temperatures. Calcium has a much higher solubility in the α′ lattice than rare-earth elements[1] and this offers great potential for controlling the proportion of grain boundary glass after sintering. Furthermore, the Ca α-sialon phase possesses excellent thermal stability; it has not transformed to the β′ phase during post-sintering heat treatment at 1450°C, unlike some of the rare earth α-sialon systems.[2,3]

Careful control of microstructural development in sialon ceramics may lessen their intrinsic brittleness. For instance, toughness is improved by promoting anisotropic grain growth of the β-Si_3N_4 and β-sialon phases, since the high aspect-ratio grains enhance crack bridging and deflection mechanisms during failure.[4,5] For the α-sialon phase, however, such control of grain morphology has not been realised, despite its similarity to β-sialon in both chemistry and crystal structure. The commonly observed grain morphology for α-sialons is equiaxed.[6] This results in relatively low toughness for the α-sialons and partly explains why the α′ phases are only found in the advanced ceramics market as the minor constituent in α′-β′ ceramic composites. In these latter materials, the higher hardness of α′ supplements the better strength and toughness of the β′ phase.[7]

Recent reports highlight the development of elongated α-sialon grains in Ca and Sm systems during uniaxial hot-pressing, wherein the preferred growth direction is normal to the hot-pressing axis.[8,9] It would be, however, more desirable to observe anisotropic grain growth in materials produced by the cheaper, pressureless sintering route. This paper details microstructural characteristics of elongated α′ grains in two pressureless sintered Ca α-sialon ceramics. The expected toughening arising from the grains' high aspect ratios offers the prospect for exploiting this anisotropic growth phenomenon to improve the toughness of α-sialon ceramics.

Experimental

Two compositions were examined. Within the Janecke prism representation of the Ca–Si–Al–O–N system, both lay on the Si_3N_4–3/2(Ca_3N_2)·3AlN–4/3(AlN·Al_2O_3) plane. The first sample, named CS3015, refers to a design composition of m = 3·0 and n = 1·5. Likewise, the name CS3618 describes a material of composition m = 3·6 and n = 1·8.

Powders of Si_3N_4 (HCST LC10), AlN (HCST Grade C) and $CaCO_3$ (Ajax) were milled for 24 h using Si_3N_4 ball media and isopropanol. After

*To whom correspondence should be addressed.

drying at 80°C, about 2 g of powders were uniaxially pressed into cylindrical pellets, followed by an isostatic cold press under a pressure of 200 MPa. The pellets were calcined for 1 h at 800°C in a nitrogen atmosphere. Then, they were packed in a powder bed of 50 wt% Si_3N_4–50 wt% BN and were pressureless sintered in a nitrogen atmosphere within a graphite furnace. A two-stage sintering procedure was employed, namely, a 1 h dwell at 1600°C followed by a 4 h dwell at 1800°C. The temperature was raised at 10°C min^{-1} to 1200°C and at 5°C min^{-1} thereafter. Samples were cooled at a rate of 10°C min^{-1}.

After sintering, bulk densities were measured via the mercury immersion method and weight losses were recorded. Some microstructural and composition differences exist between the surface and interior of each sample, which may have resulted from preferential evaporation of chemicals in the surface region. Consequently, for subsequent analyses, the materials were considered to consist of two regions, namely, the 'core' and the 'rim'. This rim region constitutes the material approximately 0·5 mm below the surface.

Hardness and toughness were measured using a Vickers diamond pyramid indenter with a 196N load.[10] Phase identification and lattice parameter measurements were performed on a Rigaku-Geigerflex X-ray diffractometer using nickel filtered, CuK_α radiation. Both phase identification and mechanical properties were recorded from polished surfaces. Lattice parameter measurements were obtained using powder samples suspended on a glass slide. Reflection positions of XRD were calibrated against those of a ThO_2 standard and were then processed via the computer program Celsiz.[11] The *m*-values for the α-sialon phases were calculated from the formulae in Ref. 12.

Microstructural characterisation was undertaken with a JEOL 840A scanning electron microscope and with Philips CM20 200 kV and Philips EM420 120 kV transmission electron microscopes. Both the JEOL 840A and the EM420 were equipped with energy dispersive X-ray spectrometers (EDXS). The SEM samples were etched in molten NaOH prior to analysis.

Results and Discussion

The X-ray diffraction traces demonstrate the predominance of the Ca α-sialon phase at the rim and core regions of both specimens (Fig. 1). No β-sialon is evident, though there is a minor constituent in the bulk of the samples, tentatively indexed as aluminium nitride. The surface regions are deficient in AlN with respect to the cores.

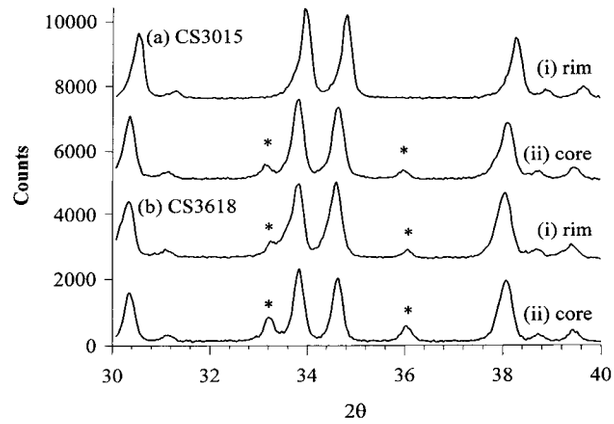

Fig. 1. X-ray diffraction traces of (a) CS3015 and (b) CS3618. Spectra were respectively collected from (i) the rim and (ii) the core regions of the specimens. The AlN peaks are labelled with '*' symbols; the remainder of the reflections belong to the α' phase.

Since the microstructural features of CS3015 and CS3618 are very similar, only the results from CS3618 are presented here. The shapes of the Ca α-sialon grains in these high m-value materials differ from the more familiar equiaxed morphology. SEM fractographs of the rim and core regions of CS3618 (Fig. 2) show high aspect ratio, elongated

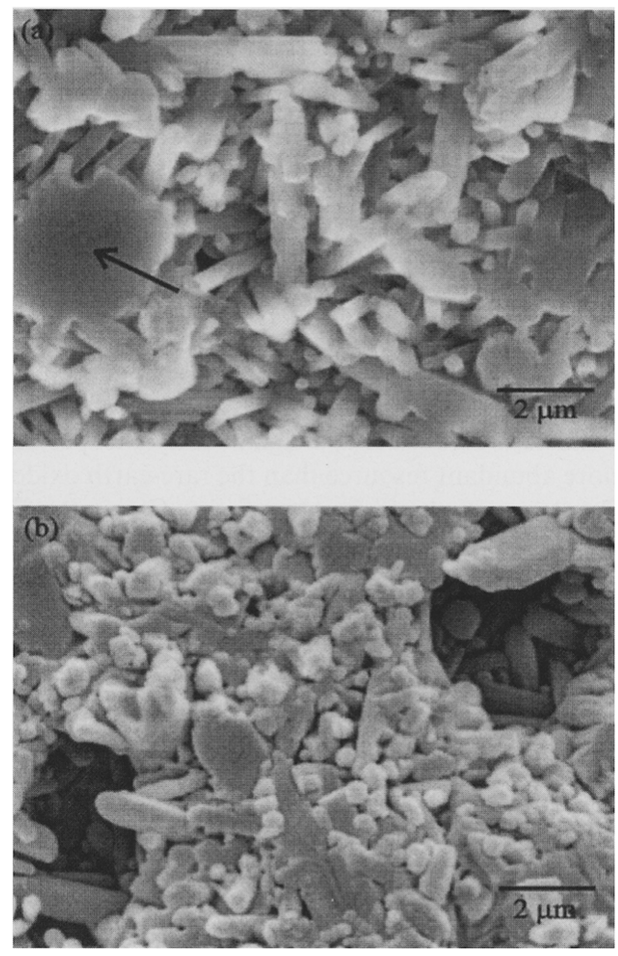

Fig. 2. SEM fractographs of the (a) rim and (b) core regions of CS3618.

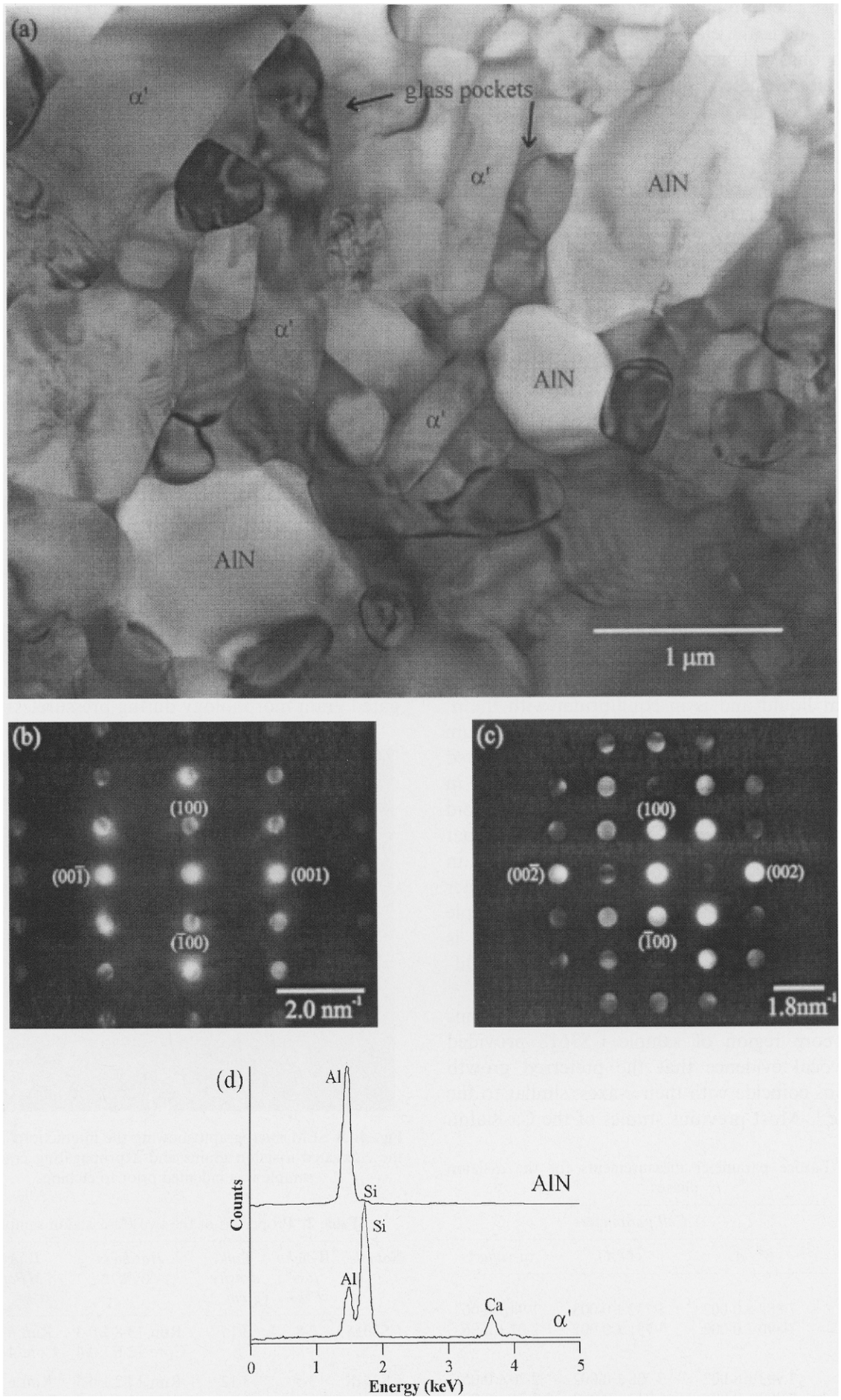

Fig. 3. (a) A bright-field image from the core region of sample CS3618, showing elongated α' grains, aluminium nitride and a grain boundary glassy phase: (b) $<\bar{1}\,2\,\bar{1}\,0>_{AlN}$ micro-electron beam diffraction pattern; (c) $<\bar{1}\,2\,\bar{1}\,0>_{\alpha'}$ micro-electron beam diffraction pattern; (d) EDXS spectra from AlN and Ca α-sialon.

α' grains. Their presence is most prominent nearer the rim. There, the elongated grains are nominally 3–6 μm long, with aspect ratios between 4–8. These results clearly indicate that with appropriate composition design and sintering procedures, the α-sialon phase may develop an elongated morphology during pressureless sintering. Isolated clusters of AlN grains were also observed, such as the one indicated by the arrow in Fig. 2(a). Phase identification was verified by EDXS analyses.

Further microstructural features are indicated in Fig. 3 (a). The TEM micrograph is of the core of CS3618. It contains the α-sialon phase, AlN and a grain boundary glass. The calcium α' is characterised by faceted, often elongated crystals, whereas the shapes of AlN grains exhibit globular morphologies. This distinction was confirmed by electron diffraction and EDXS experiments. Diffraction patterns recorded from AlN and α' are presented in Fig. 3(b) and (c), respectively. The corresponding EDXS traces are displayed in Fig. 3(d).

The small silicon content in the AlN spectrum may suggest a very low substitution of silicon into the AlN lattice, and this trace amount of silicon was not observed in the original AlN powder. This result, combining with the shape of the AlN implies that the AlN phase precipitated from the transient liquid and is in equilibrium with the α' phase under the processing conditions. In calcium α-sialon materials, higher m-value α'-phases located at the Al-rich side of the α' phase region and are in equilibrium with nitrogen rich AlN polytypoid phases. Therefore, the present results imply that the α' should have very high Al and Ca contents, in agreement with the results of the lattice parameter measurements (Table 1). The m-value for sample CS3015 is 2·0, whereas for sample CS3618, it is slightly higher (m = 2·2). There was negligible difference between the outer and inner regions.

Electron diffraction analyses of numerous α' grains in the core region of sample CS3618 provided unequivocal evidence that the preferred growth directions coincide with their c-axes, similar to the β' phase.[13] Most previous studies of the Ca–sialon system focused on the low m-values of the α' compositions in order to minimise the glass content in the samples. An increase in the m-values would lead to more liquid appearing at the sintering stage and this may facilitate the anisotropic growth of the α' phase.

From a materials processing perspective, Ca α-sialon materials are more readily prepared than most other rare-earth counterparts since they can be sintered to relatively high densities and experience little weight loss (Table 2). Interactions between the rod-like α' grains and the propagating cracks indicate the potential for toughening (Fig. 4), but the high m-value in the composition has resulted in a significant reduction in the materials hardness due to an increased amount of glass in the samples and the substitution of Al–N for Si–N bonds in the α' structure.[2]

Moreover, the differences between the core and rim microstructures affect the materials properties. The toughness values for the rim regions of both samples are notably higher than for the core regions (Table 2); the higher density of the elongated grains at the rim regions is expected to contribute to this behaviour (Fig. 2). In this light, it is suggested that α-sialons may form self-reinforced microstructures by promoting the growth of elongated grain morphology during pressureless sinter-

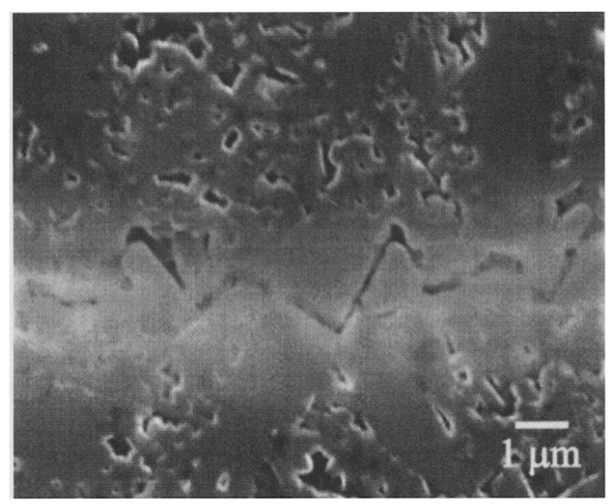

Fig. 4. A SEM micrograph showing the interactions between the elongated α-sialon grains and a propagating crack. The sample was indented prior to etching.

Table 1. Lattice parameter measurements for the α-sialon phases

Sample	*Cell parameters*		
	a*(Å)	c*(Å)	m-*value**
CS3015			
(Rim)	7·882 ± 0·002	5·732 ± 0·003	1·94 ± 0·06
(Core)	7·890 ± 0·002	5·731 ± 0·002	2·02 ± 0·06
CS3618			
(Rim)	7·903 ± 0·002	5·738 ± 0·002	2·20 ± 0·05
(Core)	7·908 ± 0·002	5·742 ± 0·003	2·26 ± 0·09

*The error bounds reflect one standard deviation in the lattice parameter measurements.

Table 2. Properties of the two Ca α-sialon samples

Sample	*Weight loss (%)*	*Bulk density (g cm^{-3})*	*Hardness (GPa)**	*Toughness (MPam$^{1/2}$)**
CS3015	2·8	3·15	Rim 13·8 ± 0·3 Core 12·6 ± 0·4	Rim 6·0 ± 0·2 Core 4·3 ± 0·3
CS3618	3·5	3·12	Rim 13·2 ± 0·3 Core 12·6 ± 0·5	Rim 6·4 ± 0·3 Core 4·2 ± 0·4

*The data ranges represent 95% confidence intervals for Student's t-distributions based on five measurements.

ing and this approach has great potential for the production of less expensive, high performance engineering ceramics. The present systems represent the first in which we have observed this growth phenomenon. The systematic tailoring of more desirable microstructures will necessitate a greater understanding of the exact processing conditions that encourage the formation of elongated α-sialon grains and the mechanism for toughening.

Conclusions

The present study has illustrated the potential for developing in-situ toughened, pressureless sintered Ca α' ceramics. High aspect ratio α-sialon crystals have resulted from the preferential growth along their $\langle 0\,0\,1 \rangle$ directions. Preliminary results suggest these particulate morphologies may toughen the materials. Further investigations are necessary if this growth behaviour is to be exploited to improve the toughness of the inherently brittle α-sialon ceramics.

Acknowledgement

This work was supported by the Australia Research Council.

References

1. Cao, G. Z. and Metselaar, R., α'-sialon ceramics: A review. *Chem. Mater.*, 1991, **3**(2), 242–253.
2. Hewett, C. L. Cheng, Y.-B., Muddle, B. C. and Trigg, M. B., Calcium sialon ceramics. In *Materials Research 96, Conference Proceedings Volume 1*. The Institute of Metals and Materials Australasia Ltd, Brisbane, 1996, pp. 101-104.
3. Mandal, H., Thompson, D. P. and Ekstrom, T., Reversible α–β sialon transformation in heat-treated sialon ceramics. *J. Eur. Ceram. Soc.*, 1993, **12**, 421.
4. Hoffmann, M. J., Analysis of microstructural development and mechanical properties of Si_3N_4 ceramics. In *Tailoring of Mechanical Properties of Si_3N_4 Ceramics*, ed. M. J. Hoffmann and G. Petzow. Kuwer Academic Publishing, London, 1994, pp. 59–72.
5. Lee, D.-D., Kang, S.-J. L., Petzow, G. and Yoon, D. N., Effect of α to $\beta[\beta']$ phase transition on the sintering of silicon nitride ceramics. *J. Am. Ceram. Soc.*, 1990, **73**, 767–769.
6. Hewett, C. L., Cheng, Y.-B., Muddle, B. C. and Trigg, M. B., Preparation of fine-grained calcium α-sialon. *J. Mater. Sci. Lett.*, 1994, **13**, 1612–1615.
7. Ekstrom, T. and Nygren, M., Sialon ceramics. *J. Am. Ceram. Soc.*, 1992, **75**(3), 259–276.
8. Wang, H., Cheng, Y.-B., Muddle, B. C., Gao, L. and Yen, T. S., Preferred orientation in hot-pressed Ca α-sialon ceramics. *J. Mater. Sci. Lett.*, 1996, **15**(16), 1447–1449.
9. Nordberg, L. O., Shen, Z., Nygren, M. and Ekstrom, T., On the extension of the α-sialon solid solution range and anisotropic grain growth in Sm-doped α-sialon ceramics. *J. Eur. Ceram. Soc.*, 1997, **17**, 575–580.
10. Antis, G. R., Chantikul, P., Lawn, B. R. and Marshall, D. B., A critical evaluation of indentation techniques for measuring fracture toughness. I, Direct crack measurements. *J. Am. Ceram. Soc.*, 1981, **64**(9), 533–538.
11. Scott, H. G., The Celsiz program. Division of Materials Science and Technology, CSIRO, Australia, 1996.
12. van Rutten, J. W. T., Hintzen, H. T. and Metselaar, R., Phase formation of calcium α-sialon by reaction sintering. *J. Eur. Ceram. Soc.*, 1996, **16**, 995–999.
13. Lai, K. R. and Tien, T. Y., Kinetics of β-Si_3N_4 grain growth in Si_3N_4 ceramics sintered under high nitrogen pressure. *J. Am. Ceram. Soc.*, 1993, **76**(1), 91–96.